Considerations for monitoring of deep circular excavations

Author 1

- Tina Schwamb, Ph.D.
- Department of Engineering, University of Cambridge, UK

Author 2

- Mohammed Z. E. B. Elshafie, Ph.D.
- Lecturer, Laing O'Rourke Centre for Construction Engineering and Technology, Department of Engineering, University of Cambridge, Cambridge, UK

Author 3

- Kenichi Soga, Ph.D., FICE
- Professor of Civil Engineering, Department of Engineering, University of Cambridge, UK

Author 4

- Robert J. Mair, CBE, FREng, FICE, FRS
- Sir Kirby Laing Professor of Civil Engineering, Department of Engineering, University of Cambridge, Cambridge, UK

Abstract (196 words)

Understanding the magnitude and distribution of ground movements associated with deep shaft construction is a key factor in designing efficient damage prevention/mitigation measures. Therefore, a large-scale monitoring scheme was implemented at Thames Water's 68 m-deep Abbey Mills Shaft F in East London, constructed as part of the Lee Tunnel Project. The scheme comprised inclinometers and extensometers which were installed in the diaphragm walls and in boreholes around the shaft to measure deflections and ground movements. However, interpreting the measurements from inclinometers can be a challenging task as it is often not feasible to extend the boreholes into ground unaffected by movements. The paper describes in detail how the data is corrected. The corrected data showed very small wall deflections of less than 4 mm at the final shaft excavation depth. Similarly, very small ground movements were measured around the shaft. Empirical ground settlement prediction methods derived from different shaft construction methods significantly overestimate settlements for a diaphragm wall shaft. The results of this study will help to inform future projects, such as the forthcoming 25 km-long Thames Tideway Tunnel with its 18 deep shafts being constructed adjacent to existing infrastructure.

List of notation

α	Inclination angle from vertical measured by inclinometer
α_{HB}	Empirical constant from New and Bowers (1994)
Δu	Difference in shape of inclinometer casing/ lateral movement
Δy	Vertical movement of soil element
A0, A180	Inclinometer reading taken at 0° and 180° orientation
A_{comb}	Combined inclinometer reading
$A_{comb,cor}$	DPE-corrected combined inclinometer reading
D	Diameter of shaft
d_{DPE}	Value of DPE
d_e	Deviation from vertical of 0.5 m measurement interval
E	Extent of settlement behind shaft wall
H	Depth of shaft
i	Variable to count of 0.5 m inclinometer measurement intervals (i = 1 at bottom)
K_0	Lateral earth-pressure coefficient at rest
R	Mid-wall shaft radius
S_{max}	Maximum settlement directly behind shaft wall
u	Shape of inclinometer casing/ cumulative deviation
z	Depth variable
z_{fix}	Second fixity point for bias error correction

Al	Alluvium
CH	Chalk formation
DPE	Depth position error
HB	Hoek-Brown

LC	London Clay
LGC	Lambeth Group Clay
LGS	Lambeth Group Sand
MC	Mohr Coulomb
MG	Made Ground
RTD	River Terrace Deposits
SHS	Strain-Hardening/Softening
TS	Thanet Sand formation
WIP	Wished-in-place

1. Introduction

In congested cities there is often no choice but to locate excavations in close proximity to existing infrastructure, and it is hence crucial to minimise excavation-induced ground movements. Designers often have to adopt conservative methods to estimate ground movements, which result in larger predictions than would probably occur in practice. Field monitoring of excavation-induced ground movements is therefore essential to increase the available field case histories considering technological developments in construction methods and to help improve the often-conservative design assumptions adopted in practice.

In recent years, excavations have become deeper due to the demand of more efficient use of underground space and advancements in construction technology. To capture the deformational response of the ground adjacent to deep excavations, subsurface instrumentation is required to extend to deeper soil layers, which increases the associated instrumentation cost disproportionately mainly due to higher drilling cost. In addition, the applicability of the monitoring devices conventionally used in practice needs to be assessed properly. For example, error accumulation over the depth of the boreholes for inclinometers will need to be assessed. If very small movements are expected, as is the case for a circular shaft with a very stiff lining installed prior to excavation, the errors can be in the same order of magnitude as the actual measured displacements.

Inclinometer manufacturers typically quote accuracies of ±6 mm for 25 m deep boreholes (Slope Indicator 2011). Mikkelsen (2003) argues that these values are conservative, as they are aggregates of random (varies in an unpredictable manner) and systematic (shifts all errors in a consistent manner) errors. The former may be corrected through statistical analysis by taking several repeated measurements. Since the random error is often very low (±1.24 mm for a 30 m deep borehole according to Mikkelsen, 2003) and labour costs are high, repeated measurements are often not taken. Systematic errors can be corrected more easily. In practice, however, systematic error correction is often not applied, apart from the standard bias correction, which is implemented in most monitoring data analysis software. At this stage, a clear separation should be made between the accuracy, repeatability and resolution of the measurement devices. Accuracy is the closeness of agreement between a measured value and the true value. Repeatability is a measure of the consistency in achieving identical measurements across multiple readings. Taking more measurements and averaging them reduces the random error. Resolution is the smallest change in the quantity being measured of a measuring instrument that gives a perceptible change in the reading.

Figure 1 shows inclinometer measurements from two circular shafts as reported by Muramatsu and Abe (1996) and Cabarkapa et al. (2003). In both cases no details on data analysis and error correction assumptions were given. While Muramatsu and Abe's (1996) data appears very smooth, Cabarkapa et al.'s (2003) lateral deflection profiles are rather noisy. In the case of Cabarkapa et al. (2003) (Figure 1b) it is also questionable whether the fixity assumption at the bottom of the inclinometer casing is valid; the final excavation level (25 mbgl) was only 7.5 m below the toe of the diaphragm wall at 32.5 mbgl. In addition, the numerical predictions in Figure 1b show a different trend: little movement at the top with significant movement of the toe of the wall. The wall toe fixity assumption in

the inclinometer could have significantly influenced the inclinometer data analyses and hence the difference between predictions and measurements.

Hwang et al. (2007) addressed the influence of the boundary conditions on inclinometer results. Assuming fixity at the bottom of the wall leads to outward wall movement (Figure 2a). Their study suggests that the first strut movement is negligible and that the wall could be assumed fixed at that point to obtain realistic wall movements (Figure 2b). This highlights that boundary conditions have to be selected carefully to obtain realistic inclinometer results.

Magnetic extensometers could also be significantly affected by the validity of the boundary condition assumption, particularly when measuring very small movements. The resolution and system precision of magnetic extensometers systems is often too coarse, and is not sufficient where the expected movements are in the range of a few millimetres. Vibrating wire rod extensometers have a much finer resolution (±0.1 mm), however require a boundary condition assumption, which if invalid, could affect the data. Manually surveyed surface pins with a resolution of around ±1 mm are reasonably accurate but may be disturbed by the construction site traffic.

This paper reports on the monitoring scheme of Thames Water's Abbey Mills Shaft F, which is an integral part of the Lee Tunnel project. With a depth of 68 m and a diameter of 30 m, it is one of the largest shafts ever built in soft ground conditions in the UK. Since London is currently undergoing several major tunnelling projects, the monitoring scheme at Abbey Mills Shaft F provided the opportunity to measure structural response as well as ground movements associated with the construction of deep diaphragm wall shafts. It was also possible to investigate whether the shaft lining behaved anisotropically due to the joints between the individual panels as proposed by Zdravkovic *et al.* (2005) and Cabarkapa *et al.* (2003). This is discussed in detail in Schwamb and Soga (2015).

The instrumentation scheme included multi-point rod extensometers, magnet extensometers, inclinometers and surface levelling pins, as well as fibre optic instrumentation embedded into the diaphragm wall lining. This paper presents details of the instrumentation, boundary conditions assumptions, error correction procedures and the monitoring results. It also highlights how future monitoring schemes could be improved to minimise erroneous data and that quality surveying data is crucial. It furthermore compares the results with an existing empirical method to validate its applicability to deep diaphragm wall shaft excavation. The fibre optic instrumentation is outside the scope of the paper and further details can be found in Schwamb et al. (2014).

2. Abbey Mills shaft construction

The ground conditions at Abbey Mills, shown in Figure 3a, follow a typical London geology. The hydrogeological conditions comprise two main aquifers; a shallow and a deep aquifer separated by the London Clay (LC) and the Lambeth Group Clay (LGC).

The primary lining of the shaft was constructed from twenty 1.2 m thick and 84 m deep diaphragm wall panels between September and December 2011 with a capping beam at the top of the wall. Excavation started in April 2012 and was completed in September 2012. Following excavation to a depth

of 73 m, a 2 m-thick base slab was built and a secondary lining was erected inside the shaft. The annulus, an approximately 0.6 m wide gap between the diaphragm wall and the secondary lining, was filled with grout in April 2013.

3. Monitoring Instrumentation

A plan view of the shaft showing the locations of the eight surface levelling pins, the inclinometer and extensometer boreholes is presented in Figure 3b. Two arrays (A and B) comprising five boreholes each radiate from the shaft behind panels P15 and P20. Each array consists of three manual inclinometers, two multi-point automatic rod extensometers and two magnet extensometers. A cross-sectional view through an array is shown in Figure 3a together with the depths of the boreholes and the anchor locations for the multi-point extensometers. In addition three manual inclinometers were installed in the diaphragm shaft wall (AI1 in panel P15, BI1 in panel P20 and CI1 in panel P20).

3.1 Levelling pins and surveying

The eight levelling pins were road nails drilled and cast into the concrete platform. They were arranged in two arrays, AMA1 and AMA2 (Figure 3b). The levels of the road nails were measured by a precise level from two stable benchmark points. This achieves an accuracy of approximately $\pm$1 mm. The survey was carried out by the main contractor and started in mid-May 2012 when the shaft excavation level had already reached 20 m below ground level (bgl).

The borehole heads of the sub-surface soil instrumentation were also surveyed by the main contractor to provide a boundary condition for the inclinometers and the extensometers. It is worth noting that the procurement and the specification for the survey work were undertaken by the main contractor.

3.2 Extensometers

Two different kinds of extensometers were used to measure subsurface movements.

The rod extensometers (AE1, BE1, AE2, BE2) were closer to the shaft and had six anchors over their depth (Figure 3a). A schematic view of one of the rod extensometer boreholes is shown in Figure 4a. The hydraulic anchors at various depths were connected to the vibrating wire displacement sensors in the reference head (Figure 4b); the connection rods between head and anchor were protected by a hollow pipe. After installation the annulus was backfilled with grout. The reference head was supported by a sandy backfill, but was essentially free to move (Figure 4a). A borehole head survey was carried out to act as reference. However these could not be used as will be detailed later in the paper.

The instrumentation cables were routed through ducts into the data logger inside a dedicated monitoring hut (Figure 3b). The ducting was embedded into the concrete platform that was cast prior to the excavation works.

The vertical movement of the anchors was measured by vibrating wire technology automatically every 5 minutes with a resolution of around ±0.1 mm.

The magnet extensometers (AE3, BE3, AE4, BE4) were installed further away from the shaft. The spider magnet anchors were attached around an inclinometer casing (Figure 4c and d), which allowed

the borehole to be used for both, magnet extensometer and manual inclinometer. Each borehole had between 4 and 6 spider magnets over its depth and was interrogated manually once a week. Typically, a magnet sensor connected to a measurement tape was lowered into the borehole. When the sensor passed the magnet field of a spider magnet a beep sound informed the technician to read from the measurement tape using the top of the casing as reference. Each spider magnet has two magnet zones, one slightly above and one slightly below the centre of the spider magnet. At Abbey Mills the operator consistently noted the depth of the upper magnetic field. The measurement tape had a resolution of around 10 mm, and the accuracy with which values could be read off the tape was approximately ± 5 to 10 mm.

The extensometer installation and data collection were carried out by a specialist instrumentation contractor. Data collection started in August 2011 before the diaphragm wall construction and continued throughout shaft excavation until June 2013.

It should be noted that the instrumentation operators only took single measurements on the magnet extensometers and that the repeatability could be an issue. Repeatability is quoted as ±3 to 5 mm (Slope Indicator, 2013), and this range was verified by the first author who conducted an exercise to check the repeatability. However, this result is only achieved with extreme care and diligence.

3.3 Inclinometers

As shown in Figure 3b, three inclinometers were installed in the diaphragm wall (AI1, BI1 and CI1), while six borehole inclinometers were installed in the surrounding ground (AI2, AI3, AI4, BI2, BI3 and BI4). All three shaft inclinometers were supposed to extend to the full depth of the wall (84 m). Unfortunately for panels P10 and P15 the hollow tubes, in which the inclinometer casings were inserted after concreting of the diaphragm wall panels, were blocked with concrete at a depth of 78 mbgl and 60 mbgl. The soil inclinometers extended to their full depth as shown in Figure 3a.

All boreholes were interrogated with a manual inclinometer probe once a week between August 2011 and June 2013. This paper presents data from the shaft excavation between April 2012 and September 2012.

The survey of a borehole consisted of two subsequent inclinometer probe passes. For the A0 pass the upper wheel of the inclinometer pointed towards the shaft. For the A180 pass the probe was rotated by 180°. Combining both readings cancelled the probe's bias (zero-offset when the probe is vertical), which could shift between surveys; further details can be found in Mikkelsen (2003).

It should be noted that the instrumentation operators only took single measurements, as such the repeatability of the measurements could be an issue. Repeatability is quoted as ±0.01% Full Scale (FS) (Slope Indicator, 2011). This does however not take repeatability between different operators into account, just the instrument readout repeatability.

4. Lateral movements - Inclinometer data

4.1 Data Processing

The two subsequent passes provide the *A0(i)* and *A180(i)* reading for each 0.5 m interval *i* of the borehole (*i* = 1 at bottom). The combined reading $A_{comb}(i)$ can be obtained by [*A0(i) - A180(i)*]/2. $A_{comb}(i)$ can be converted into inclination angle $\alpha(i)$ and deviation $d_e(i)$. Adding the deviation values over the depth of the borehole, assuming no movement at the bottom of the inclinometer borehole, gives the shape of the inclinometer casing over depth *z*, *u(z)* (also termed the cumulative deviation). The lateral movement between two surveys $\Delta u(z)$ is the difference between their *u(z)* profiles.

As an example, the uncorrected inclinometer data of one borehole AI3 15 m behind the shaft wall is plotted in Figure 5a. The lateral movement profiles of surveys at four different excavation depths (15, 35, 53 and 71 mbgl), with respect to the baseline at 0 mbgl, are displayed. The data suggests unrealistic movements at depth (e.g. the spike at 42 mbgl) and inconsistent directions of movement. This is primarily due to error accumulation during the integration step which can be corrected.

4.2 Error correction

The magnitude of the movements measured at Abbey Mills shaft was very small (see Section 4.3), which resulted in a high signal-to-noise-ratio and the measurements to be within the accuracy of the measurement system. However, it is possible to correct for errors as discussed in detail below.

Several errors can cause systematic errors. According to Mikkelsen (2003) sensitivity drift is the least common error, but is often the most devious error to notice. Rotation error can occur when the borehole has significant inclinations in the B-axis direction, which is not the case at Abbey Mills shaft.

Bias shift is the most common systematic error experienced in inclinometer measurements. It occurs when the probe's bias shifts between the A0 and A180 passes and it causes the profile to rotate around the bottom fixity point (Mikkelsen, 2003). It can be corrected easily, if apart from the bottom of the casing a second fixity point z_{fix} is known, e.g. if the bottom section of the casing is embedded in stable ground. Then the lateral displacement profile is rotated around the bottom fixity point so that $\Delta u(z_{fix}) = 0$. For shallow excavation stages, it is possible to fix a section of the casing below excavation level where no movement would be expected as shown in Figure 6 for the 62 mbgl survey of a shaft inclinometer.

At deeper excavation stages, however, the bottom of the casing is likely to move and cannot be assumed fixed. This is because the inclinometer boreholes placed in the soil are shorter than the maximum excavation level as shown in Figure 3a. Hence the bias correction, as conventionally done in practice, could not be applied.

To conduct bias-correction on the shaft inclinometer data at deeper excavation levels, it was possible to assume fixity at the top of the wall due to the presence of the stiff capping beam. This procedure is explained in Figure 6. The 62 mbgl excavation survey is bias-corrected with a second fixity point below excavation level as detailed above. For the 71 mbgl survey this was not possible anymore and hence it was instead assumed that no significant additional movement occurred at the top of the wall,

so that the movement at the top is the same as the previous survey: $\Delta u_{71}(0)=\Delta u_{62}(0)$. The second fixity point z_{fix} was picked at around 20 mbgl and it was also assumed that $\Delta u_{71}(z_{fix})=\Delta u_{62}(z_{fix})$. It should be pointed out that this procedure is very sensitive to the choice of the location of the fixity points.

Depth position error (DPE) may also occur when the borehole is not installed straight, but in a wavy shape such as in Figure 5b. Errors are induced if the probe's position during a survey is slightly above or below its position compared to the reference survey.

Figure 5b shows the measured shape of borehole AI3, showing a wavy shape as well as an offset between the two ends of approximately 1 m which is caused by the limits of the verticality control during drilling. The wavy shape usually occurs if the casing is restrained from the top to resist the uplift force from the fluid concrete during grouting of the borehole. Due to this casing shape, the deviation values $d_e(i)$ are large and fluctuate as shown in Figure 5b. Comparing this profile with the uncorrected lateral movement profiles (Figure 5a), some features, such as peaks and bulges are congruent; this is a clear identification that DPE has occurred.

The combined uncorrected reading $A_{comb}(i)$ can be corrected as follows,

$$A_{comb,cor}(i) = A_{comb}(i) + \left(A_{comb}(i \pm 1) - A_{comb}(i)\right) \cdot \frac{|d_{DPE}|}{500mm} \qquad (1)$$

If the probe's position was lower than in the initial survey, the reading below A_{comb}(i-1) is used in Equation 1; if the position is higher, the reading above A_{comb}(i+1) is used instead. The corrected readings $A_{comb,cor}(i)$ are then used to obtain inclination angle, deviation and hence lateral deflection profiles.

Finding the correct value of d_{DPE} is elaborate and time-consuming as the exact depth offset is often not known. Through trial and error a suitable value for d_{DPE} can be approximated. In this study, each reading was plotted with a range of different d_{DPE} values. An example for the survey taken at 53 mbgl for borehole AI3 is shown in Figure 5c. The corrected profiles with d_{DPE} values ranging from -60 mm to +20 mm are plotted in the figure. It can be seen that the bulges and spikes observed at depths disappear, but increase significantly towards the top. If instead a linear variation of d_{DPE} with depth is assumed (maximum value d_{DPE} at the bottom, linearly reducing to zero at the top) the results are more reasonable. With the bottom of the borehole being further away from the top reference point the linear assumption can be justified. It is however difficult to state the exact reason for the changes in depth, but from the similar shapes of the uncorrected lateral deflection (Figure 5a) and the deviation profile (Figure 5b) DPE occurrence and its correction is justified.

From Figure 5c it can also be seen that some regions of the deflection profile tend to be more prone to DPE, while others were not influenced by the d_{DPE} value. For the bias correction it was aimed, when possible, to pick z_{fix} in a region not affected by the d_{DPE} value, e.g. in this case 32.5 mbgl.

The updated profile (after accounting for bias and depth position errors) is shown in Figure 5d. The lateral ground movement at the top increased to a maximum of 3.5 mm when the excavation reached 71 mbgl, close to formation level. The updated deflection profiles are more reasonable compared to

the uncorrected profiles shown in Figure 5a. The table in the figure shows the assumptions that were made for d_{DPE} and z_{fix}. For the deepest survey (at 71 mbgl excavation depth) it was not possible to pick a fixity point z_{fix} for bias correction, as the excavation depth was deep below the bottom of the borehole AI3.

Please note that the results are highly dependent on the error correction assumptions.

4.3 Horizontal lateral movements of the wall and ground

This paper presents the excavation-induced lateral wall and ground movement. The lateral movement of five inclinometers are plotted at three different excavation stages in Figure 7. Each subfigure plots the three shaft inclinometers (AI1, BI1 and CI1), two soil inclinometers (AI2 and BI2 situated 6 m behind the shaft wall as shown in Figure 3b) as well as the numerical predictions obtained from a numerical parametric study using FLAC2D.

The numerical analyses adopted an axisymmetric model 93 m in width and 120 m in depth with around 13000 elements of approximately 1 m x 1 m element size. The diaphragm wall was modelled with solid elements and was wished-in-place (WIP); installation effects were taken into account with reduced K_0 values. An uncoupled modelling approach was used with effective-stress based soil models. An elastic plastic Mohr-Coulomb (MC) model was adopted for the MG and the RTD. The clay layers (LC and LGC) were also modelled with the MC model but in addition a hyperbolic stiffness degradation function was implemented to simulate non-linear behaviour before yield. The LGS and the TS were modelled with the Strain-Hardening/Softening (SHS) model, the Hoek-Brown (HB) model was used for the Chalk. Input parameters are displayed Table 1; further details can be found in Schwamb and Soga (2015).

Figure 7a shows small cantilever-like horizontal wall movements of approximately 2 mm at the top of the diaphragm wall during earlier excavation stages (21 mbgl), while the FLAC model calculates no movement at the top and a bulge at depth. The measurements indicate that the soil 6 m behind the wall did not undergo any significant horizontal movements, while FLAC calculated approximately 1 mm horizontal movement.

With increasing excavation depth (47 mbgl, Figure 7b) the shaft wall inclinometer measurements agree well with the numerical calculations, both showing a sharp bulge at the excavation level just above the Chalk. The horizontal ground movement profile exhibits a small bulge (about 1 mm maximum), approximately half of the value calculated by FLAC.

At the final measurement at an excavation stage of 71 mbgl (Figure 7c) the measured maximum wall deflections are less than 4 mm, which agreed well with the FLAC results. The measured ground movement does not match the numerical calculations due to the inclinometer boundary conditions assuming a stable bottom of the borehole, while the FLAC data shows movement towards the shaft.

The error correction procedure as detailed in the previous section was vital to obtain reasonable deflection profiles. Without the DPE and the bias correction wall deflections would have been significant-

ly overestimated with values up to ±15 mm; in addition, erratic shapes and non-gradual movement would have been unavoidable.

In summary, the lateral horizontal deflection of the wall was characterised by very small bulging of the wall at depth with a maximum wall deflection of less than 4 mm. The ground in close proximity to the wall had a very similar horizontal displacement profile with the displacements considerably smaller in magnitude (1 mm maximum at depth).

While inclinometer data was also taken during diaphragm wall installation, this data could not be used. It was not possible to assume the bottom of the borehole to be fixed, as the panel depth of 84 m was deeper than the inclinometer boreholes (Figure 3a). Unfortunately, the high drilling costs associated with deeper boreholes limited the depth.

4.4 Short comings and lessons learned

The following lessons were learned from the Abbey Mills inclinometer data and it is recommended to address these issues for future instrumentation schemes:

- When very small movements are expected, the accuracy and resolution of the inclinometer system (and indeed any measurement system) have to be reviewed carefully in relation to the expected movements.
- Random error could be reduced by taking multiple readings per borehole and averaging them.
- The systematic DPE could be reduced by installing the casing as straight as possible. During the grouting stage, the casing should not be restrained from the top during grouting, but instead the bottom should be anchored into the ground (or weights added at the bottom).
- The systematic bias error can be corrected more reliably if the inclinometer casings are extended below the excavation level into stable ground.

5. Vertical movements

5.1 Soil settlement measured by rod extensometers

The rod extensometers measured relative movement between the borehole heads at the soil surface and the anchors that were installed at varying depths (Figure 3a). To obtain the total settlements, borehole head surveys were carried out. However, the surveys yielded results with a high noise level of approximately 5 mm and could not be used. Hence, the bottom anchors at approximately 70 mbgl for AE1 and BE1 and at 54 mbgl for AE2 and BE2 were assumed to act as stable references. This is to compensate for any movement of the reference head, which was essentially free to move.

The subsurface settlement results, relative to the deepest anchor, are presented in Figure 8, for the four boreholes (AE1, AE2, BE1 and BE2). The graphs also include the construction activities. It can be seen that the diaphragm wall construction from September to December 2011 caused large settlements in Array B (Figure 8c and d), a maximum of 6 mm at the shallower anchors. In Array A smaller values of around 2 mm are recorded (Figure 8a and b). After diaphragm wall construction, several abrupt settlements occurred in AE2; these might have been caused by friction between the

extensometer rods and the sleeves that house them with a suddenly release at a number of occasions.

Figure 8 shows that very small incremental settlements of only around 1 mm were recorded during the shaft excavation. This highlights that the majority of ground settlement around a diaphragm wall shaft occurs during the wall construction with the shaft excavation itself causing only very small ground settlement. This can be attributed to the stiff circular structure of the shaft with very good construction joints between the diaphragm wall panels. The primary panels were constructed first and when the secondary interjacent panels were excavated the hydrofraise machine cut into the concrete of the primary panels so that direct contact was guaranteed (also see Schwamb and Soga, 2015). Due to these stiff joints, the insitu lateral earth pressures were mainly taken by hoop stresses and the wall exhibited very small deflections as shown in Figure 7, which in turn resulted in very small ground movement.

In the two months after the completion of the excavation additional settlement (around 2 mm) was recorded in the shallower sensors. It is interesting to note that the annulus infill (gap between diaphragm wall and secondary lining) resulted in a small heave of around 1 mm.

5.2 Magnet extensometer data

The extensometer boreholes further away from the shaft (AE3, AE4, BE3 and BE4) were manual magnet extensometers with an operator taking measurements manually using a probe at set time intervals. These measurements obtained at the different stages of construction (not displayed) were very noisy between ±10 mm and showed no particular trend. This shows that the resolution of the system was not good enough to produce reliable measurements of small displacements of less than 10 mm.

5.3 Optical surface settlement survey data

The results from the surface levelling pins are displayed in Figure 9 separately for each array. Unfortunately any settlement prior to June 2012 at early excavation stages was not captured, as the survey only started at an excavation level of 20 mbgl.

The surface settlement is insignificant during shaft excavation, which shows that very small surface settlement occurred during excavation between 20 and 71 mbgl, which is in line with the observations from the rod extensometers (Figure 8). Some targets (6000, 6001, 6102 and 6103) have undergone additional settlement after completion of the excavation process. The location of these pins is close to the site traffic routes and the crane locations as shown in Figure 3b, while the area north west of the shaft around targets 6100 and 6101 was only used for storage, which may suggest that the settlement was influenced by site traffic.

5.4 Comparison to other field data, empirical and numerical predictions

For the estimation of ground settlements during the design stage, British practitioners often rely on the case study by New and Bowers (1994) who measured surface settlement around an access shaft of diameter D = 11 m and depth H = 26 m built for the Heathrow Express trial tunnel. It was constructed

in London Clay using caisson and underpinning methods at shallow depth. Subsequently, at greater depths, the shaft was excavated in 1 m steps and then lined with shotcrete (Deane and Bassett, 1995).

New and Bowers (1994) fitted a trendline to their measurements to obtain the surface settlement S_v at a distance d behind the shaft,

$$S_v(d) = \frac{\alpha_{NB}(H-d)^2}{H} \qquad (2)$$

where α_{NB} is an empirical constant; the value of 6 x 10^{-4} best fit their data. New and Bowers (1994) acknowledge that this formula may only be applied to shafts with similar dimensions, and state that different values for α are needed to adjust for different construction methods and ground conditions. However, the literature does not contain any further values for α.

In practice, due to limited available field studies, designers and third parties sometimes use New and Bowers' (1994) measurements and their engineering judgement to produce settlement estimation guidelines for tunnelling projects.

When applying New and Bowers' formula to the Abbey Mills shaft, the results show a maximum settlement of 41 mm (0.06% *H*) next to the shaft wall with the displacements extending 68 m (1*H*) behind the diaphragm walls. Figure 10 contains the normalised New and Bowers' formula (settlement is indicated by positive values, heave by negative values).

Figure 10 also contains the normalised field measurements from the highest anchor of the rod extensometers (at around 8 mbgl) used here as an approximation of the surface settlement. The maximum settlement of the shallowest anchor of all four rod extensometer boreholes during diaphragm wall installation (+) and during shaft excavation (x) are plotted. It can be seen that the values are very small, not exceeding 0.007% *H* (≈ 5 mm) and hence the empirical constant in New and Bowers' formula could be significantly smaller when diaphragm walls are used in similar circumstances, or the formula could be inapplicable to this type of construction.

Surface settlement measurements from another diaphragm wall excavation with *D* = 28 m and *H* = 60 m, similar to Abbey Mills, are also plotted in Figure 10 (Muramatsu and Abe, 1994). It can be seen that the measurements are of similar magnitude as those measured at Abbey Mills, supporting that diaphragm wall shafts are significantly stiffer than shafts using caisson and underpinning methods, and that therefore New and Bowers' formula is not applicable. It should be noted, however, that Muramatsu and Abe's study was conducted in Japan in layered ground consisting of gravel and loam, very different to London ground conditions, and may therefore not directly applicable to shafts in London.

Figure 10 also includes the normalised numerical results which show heave of approximately -0.007% *H* (≈ 5 mm) behind the shaft wall. This calculation is supported by the results from the eight targets which were attached to the diaphragm wall head shown in Figure 11. The top of the wall heaved gradually during excavation; at the final excavation stage between 7 and 10 mm heave were

measured. The plot of displacement vectors from the numerical model (Figure 12) shows that this heave originated from the removal of overburden pressure on the excavation surface. This caused the wall as well as the adjacent ground to heave and also affected the bottom anchor of the rod extensometers, which moved upwards by approximately 3 mm. Hence, the assumption of a stable bottom anchor for the rod extensometers becomes questionable. The rod extensometer results from the shaft excavation (Figure 8) therefore only show relative movement between the bottom anchor and the ones above. A more accurate and real-time borehole head survey would have been needed to be able to measure absolute soil settlement/heave. Alternatively, the borehole would need to extend much deeper, approximately 30 to 40 m below the final excavation depth to be able to assume a stable bottom anchor. This would however increase the costs of drilling significantly.

From a damage risk point of view, however, the important message is that all measurements clearly indicated that very small soil displacements were associated with the shaft excavation at the Abbey Mills shaft. Even though the settlements measured during diaphragm wall construction were larger than those during excavation, the overall movements were generally very small for practical reasons.

5.5 Shortcomings and lessons learned

The authors would like to comment that, in general, the survey data collected for this project was not sufficiently accurate when compared to the small measurements recorded during shaft excavation. As such, the following shortcomings and lessons were learned from the survey of vertical movements at Abbey Mills:

- Automatic rod extensometers require a reliable and accurate enough boundary condition. This may be achieved by either extending the boreholes into ground strata unaffected by ground movements or by employing a more accurate and frequent head survey. If the head survey option was adopted, special attention should be given to the survey specifications; better accuracy could be achieved by adopting tighter specifications.
- Magnet extensometers should not be used if small movements of less than 10 mm are expected. If movements are within or above this range, a mm-graduated tape and a reliable procedure to read off the tape should be used.
- The repeatability of all instruments can be improved by increasing the number of readings and averaging them.

6. Conclusions

This paper has presented the results from the monitoring scheme implemented at Thames Water's Abbey Mills Shaft F in East London. The results from inclinometer, extensometer and conventional survey data are presented and compared to numerical and empirical calculations. It was detailed how the inclinometer readings were corrected for systematic errors. The findings with regard to mechanism of the movement of the wall and the surrounding ground are summarised below. It is to be noted that the surface surveying data was not sufficiently accurate when compared to the small ground movements that occurred during construction. The findings below will have to be viewed bearing this in mind:

1. Consistently, all data showed that very small wall and ground movements occurred during the 73 m deep shaft excavation. Initially, during early shaft excavation stages, the wall showed small cantilever-like movements and then bulged at depth where the maximum wall deflection recorded was less than 4 mm, which is in good agreement with the numerical calculations. The excavation-induced maximum horizontal ground movements were around 2 mm. Please note that these values do not include the ground movement during diaphragm wall construction which could be of similar or lager magnitude. These measurements were taken but could not be error corrected due to missing boundary conditions.
2. Maximum ground settlement at the surface was around 8 mm during diaphragm wall construction. During shaft excavation, it seems likely that heave of around 5-10 mm occurred due the removal of overburden pressure inside the shaft causing soil around the shaft to heave. Overall, the ground movement was very small.
3. Empirical predictions of vertical ground movement using an equation based on field data from a shaft, constructed with underpinning methods, gave very large settlements, up to 40 mm. At Abbey Mills, diaphragm walls that extended deep into the Chalk layer were installed prior to shaft excavation and consequently very small ground movements were measured. Therefore the empirical equation, as suggested by New and Bowers, should be used carefully taking into account the construction method and the ground conditions, or may not be directly applicable. In order to come up with modified empirical method, more field data of circular shaft excavation using diaphragm walls in similar ground conditions is needed.

This paper has highlighted that instrumentation of deep excavations needs to be carefully planned to make sure that boundary conditions are fully taken into account and errors are minimised. Some considerations for future monitoring schemes are summarised below:

1. If expected movements are small and boreholes are deep, inclinometers can easily accumulate errors that are larger than the movement they are required to measure. This study showed how the data can be corrected to compensate for bias and depth position errors. The latter can be minimised by installing the casing as straight as possible, and using the same probe, cable and technician. Bias error requires the assumption of a stable section of the inclinometer casing. Therefore instrumentation boreholes should be specified to be extended approximately 10 m deeper than the final excavation depth into ground strata unaffected by ground movement. If possible it is also recommended to take multiple readings which can be averaged to reduce random error and improve repeatability.
2. Automatic vibrating wire rod extensometers proved to be reliable with very small resolution; however they require a boundary condition of known movements. Optical borehole head surveys are often not accurate enough when small movements are expected and assuming a stable bottom anchor is not always valid. Hence it is recommended to make sure that a more accurate and frequent head survey is conducted (this may be achieve through tighter specifications), or to extend boreholes deeper into ground strata unaffected by ground movement. Inclinometers would also benefit from an accurate survey of the borehole head.

3. The magnet extensometers system used at Abbey Mills did not provide good enough resolution for the small movements. For future sites where small movements (less than 10 mm) are expected, it is recommended to use a millimetre-graduated tape, to use a reliable procedure to read off the tape, and to take number of readings which can be averaged.

Overall, this work has shown that the Abbey Mills shaft behaved in a very stiff manner and caused minimal ground movements around it; this is directly relevant to the construction of deep shafts planned for forthcoming tunnelling projects if they are to be constructed with diaphragm walls.

Acknowledgements

The authors would like to thank Thames Water Ltd and the Lee Tunnel Project Management Team for making the field study possible; the support from Richard Sutherden, John Greenwood, Roger Mitchell and Peter Jewell is greatly appreciated. The authors would also like to acknowledge the support received from SolData Ltd during the installation of the instrumentation and data acquisition stages of the project. The assistance and help from the contractor MVB JV (a joint venture of Morgan Sindall, Vinci Construction Grands Projets and Bachy Soletanche) were essential for the successful accomplishment of the field study; special thanks go to Ba Dan Nguyen, Clotilde Boquet, Jean-Christophe Galan, Julian Gatward and Sivilay Sayavong. The financial support from the EPSRC UCL - Cambridge Centre for Doctoral Training in Integrated Photonic and Electronic Systems (CDT IPES) and the George and Lillian Schiff Foundation is also greatly acknowledged.

References

Cabarkapa, Z., Milligan, G. W. E., Menkiti, C. O., Murphy, J., and Potts, D. M. (2003). “Design and performance of a large diameter shaft in Dublin boulder Clay.” *Proc., BGA Int. Conf. on Foundations*, T. A. Newson, ed., Thomas Telford Ltd., London, 175–185.

Deane, A.P., and Bassett, R.H. (1995). “The Heathrow Express Trial Tunnel.” Proc., ICE - Geotechnical Eng., 113(3), 144–156.

Dunnicliff, J. (1988). Geotechnical Instrumentation for Monitoring Field Performance, John Wiley & Sons, New York.

Hwang, R. N., Moh, Z., and Wang, C. H. (2007). “Toe Movements of Diaphragm Wall and Correction of Inclinometer Readings”. *J. of GeoEng.*, 2(2), 61–71.

Mikkelsen, P. E. (2003). “Advances in Inclinometer Data Analysis.” *6th Int. Symp. on Field Measurements in Geomechanics (FMGM 2003),* F. Myrvoll, ed., Swets & Zeitlinger B.V., Lisse.

Muramatsu, M., and Abe, Y. (1996). “Considerations in shaft excavation and peripheral ground deformation.” *Geotechnical Aspects of Underground Construction in Soft Ground*, R. J. Mair, and R. N. Taylor, eds., Balkema, Rotterdam, 173–178.

New, B. M., and Bowers, K. H. (1994). “Ground movement model validation at the Heathrow Express trial tunnel.” *Proc. 7th Int. Symp Tunnelling ’94, London,* 301–329.

Schwamb, T. Soga, K., Mair, R. J., Elshafie, M. Z. E. B., Sutherden, R., Boquet, C., and Greenwood, J. (2014). “Fibre optic monitoring of a deep circular excavation.” *Proc., ICE - Geotechnical Eng.*, 167(2), 144–154.

Schwamb, T., and Soga, K. (2015). “Numerical Modelling of a Deep Circular Excavation at Abbey Mills in London.” Géotechnique, accepted for publication, DOI: 10.1680/geot./14-P-251

Slope Indicator (2011). “Digitilt Inclinometer Probe.” Datasheet. Available at: http://www.slopeindicator.com/pdf/digitilt-vertical-inclinometer-probe-datasheet.pdf [Accessed 18 Nov 2014].

Slope Indicator (2013). “Magnet Extensometer.” Datasheet. Available at: http://www.slopeindicator.com/pdf/magnet%20extensometer%20datasheet.pdf [Accessed 30 Jul 2015].

Zdravkovic, L., Potts, D. M. & St. John, H. D. (2005). Modelling of a 3D excavation in finite element analysis. Géotechnique 55, No. 7, 497–513.

Figures

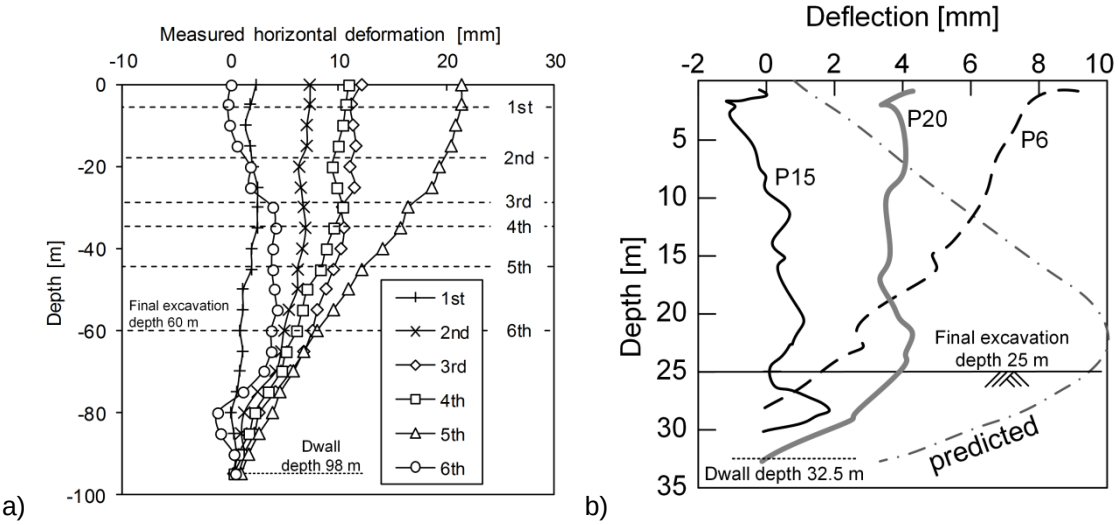

Figure 1 – Inclinometer measurements: a) Diaphragm wall deflections at various excavation levels (re-produced from Muramatsu and Abe, 1996), b) Diaphragm wall panel deflections at an excavation level of 25 m (reproduced from Cabarkapa et al., 2003)

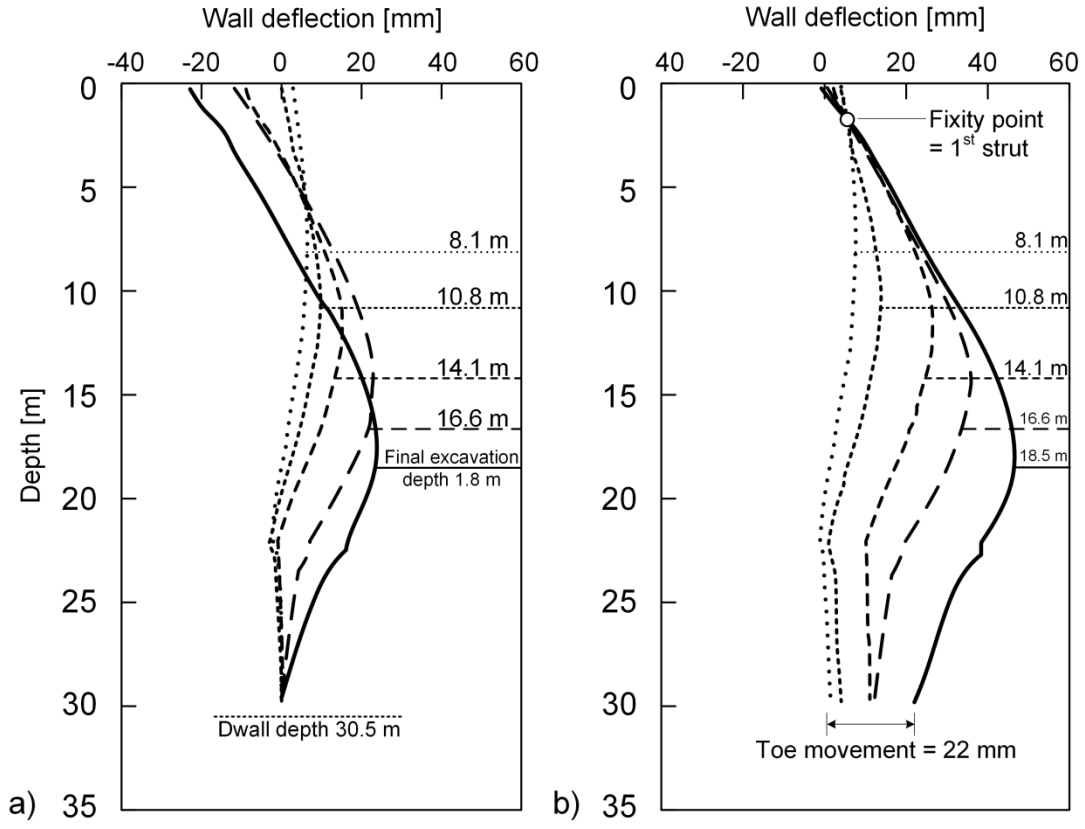

Figure 2 – Processed inclinometer data: a) assuming the toe of the inclinometer fixed, b) assuming the movement at 1st strut level constant (reproduced from Hwang et al., 2007)

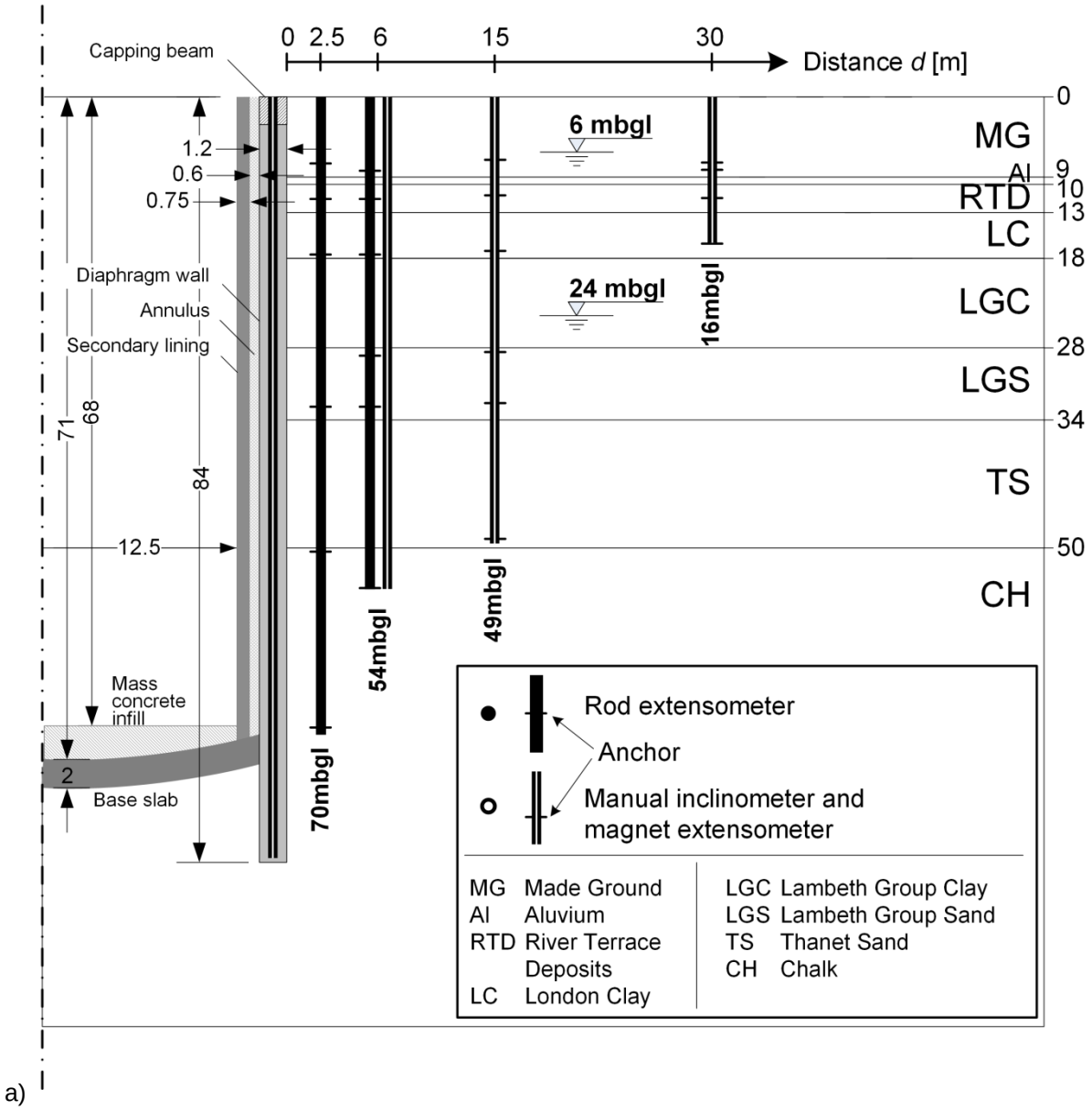
Capping beam
0 2.5 6 15 30
Distance d [m]
1.2
0.6
0.75
Diaphragm wall
Annulus
Secondary lining
71
68
84
12.5
Mass concrete infill
2
Base slab
70mbgl
54mbgl
49mbgl
16mbgl
6 mbgl
24 mbgl
MG
Al
RTD
LC
LGC
LGS
TS
CH
0
9
10
13
18
28
34
50
Rod extensometer
Anchor
Manual inclinometer and magnet extensometer
MG Made Ground
Al Aluvium
RTD River Terrace Deposits
LC London Clay
LGC Lambeth Group Clay
LGS Lambeth Group Sand
TS Thanet Sand
CH Chalk

a)

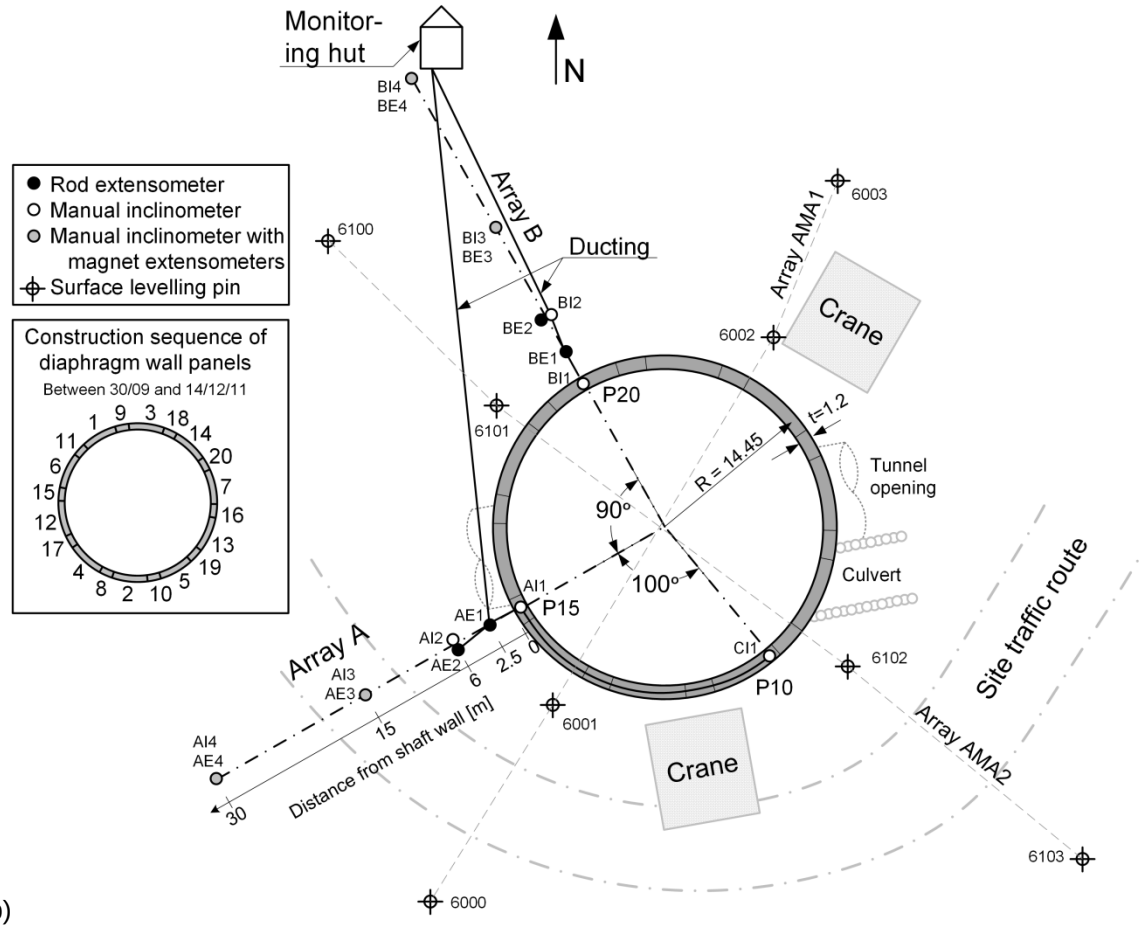

b)

Figure 3 – a) Ground strata with cross-section through structure and monitoring boreholes, b) Plan view of Abbey Mills shaft with dimensions

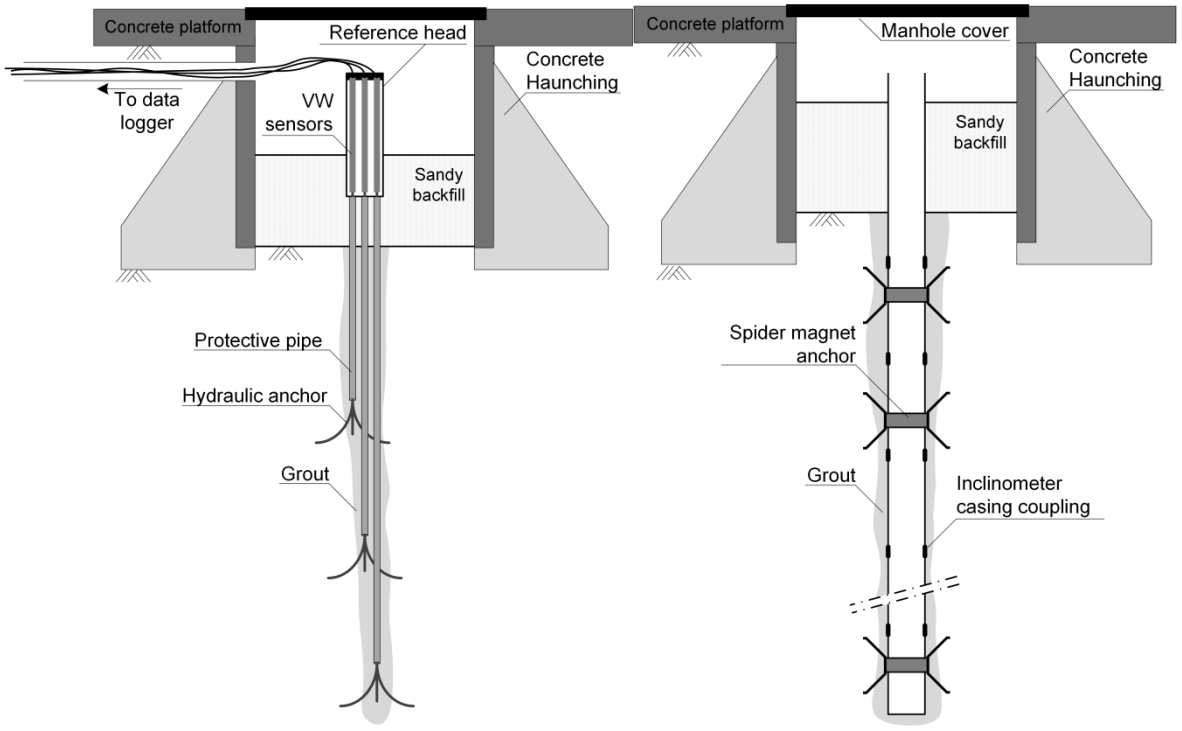

(a) (c)

(b) (d)

Figure 4 – a) Schematic view of rod extensometer borehole, b) Photograph of reference head, c) Schematic view of magnet extensometer borehole, d) Photograph of spider magnet anchor (http://nvm.ie/products/geo-xm-magnetic-settlement-systems/ Accessed 04 April 2016)

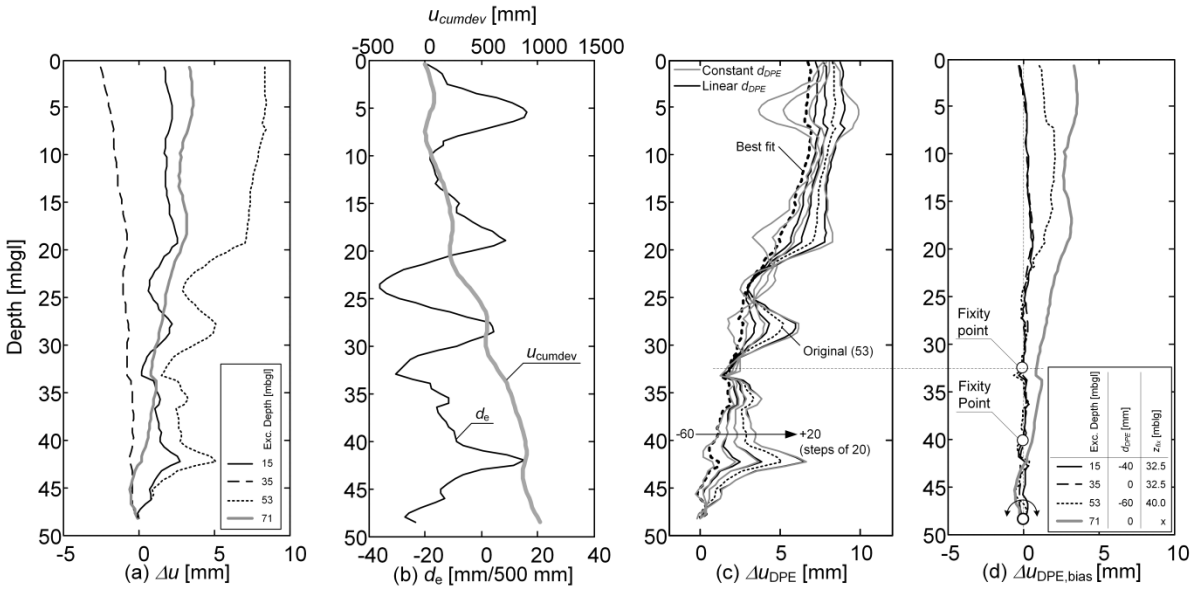

Figure 5 – Data from inclinometer AI3: a) uncorrected lateral deflection or incremental deviation of several surveys, b) borehole shape and deviation of baseline reading, c) Assuming various d_{DPE} values for the 53 mbgl survey, d) error corrected lateral deflection of several surveys

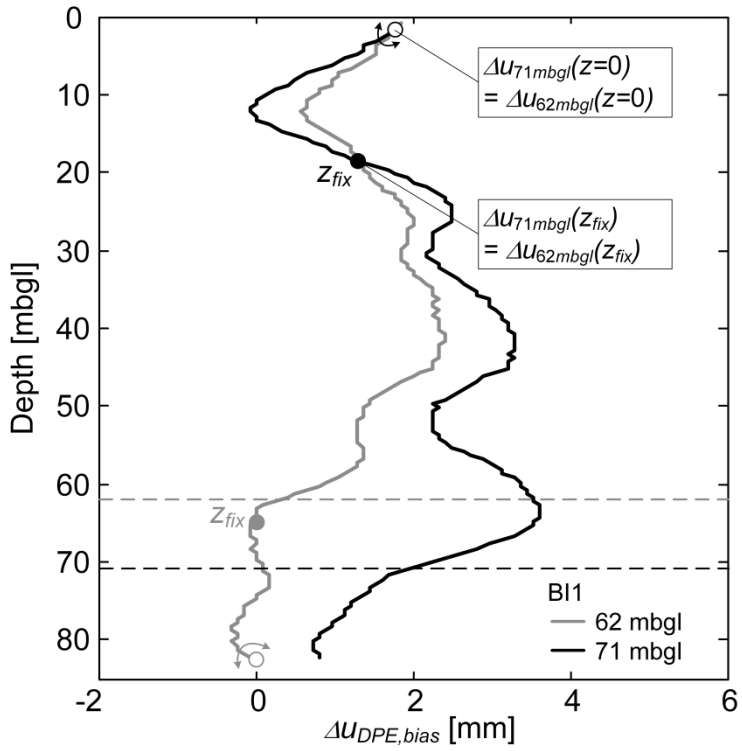

Figure 6 – Shaft inclinometers bias correction

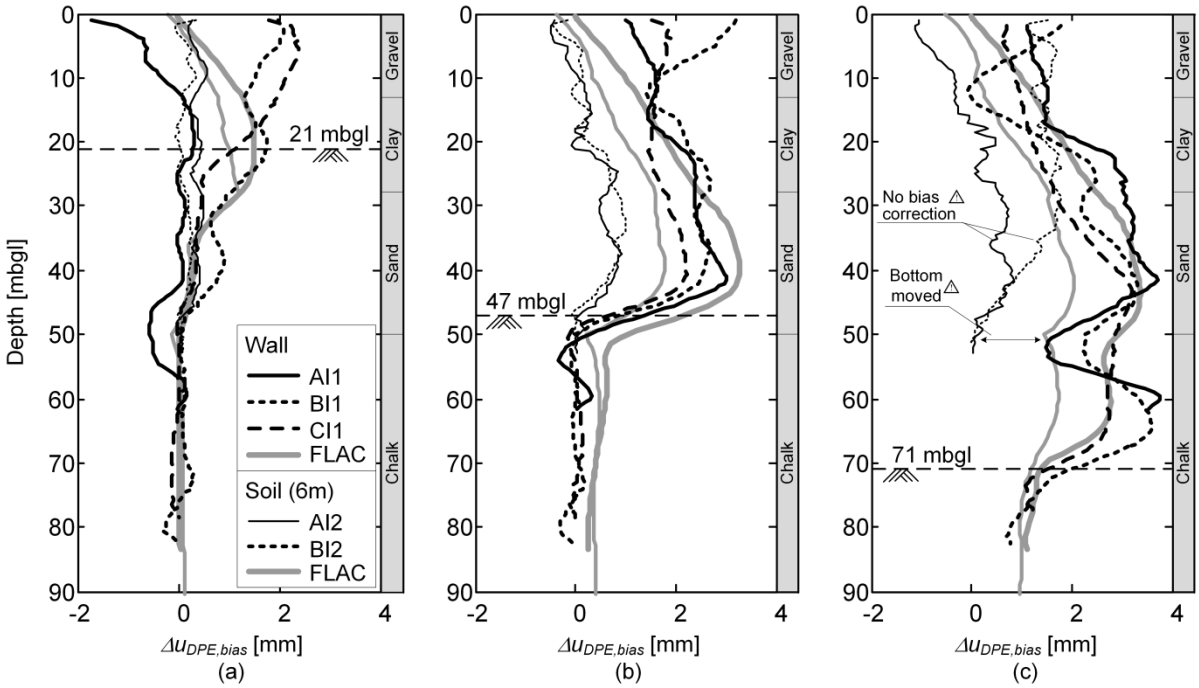

Figure 7 – Error corrected inclinometer data for the shaft inclinometers and two soil inclinometers at and excavation level of (a) 21 mbgl, (b) 47 mbgl and (c) 71 mbgl

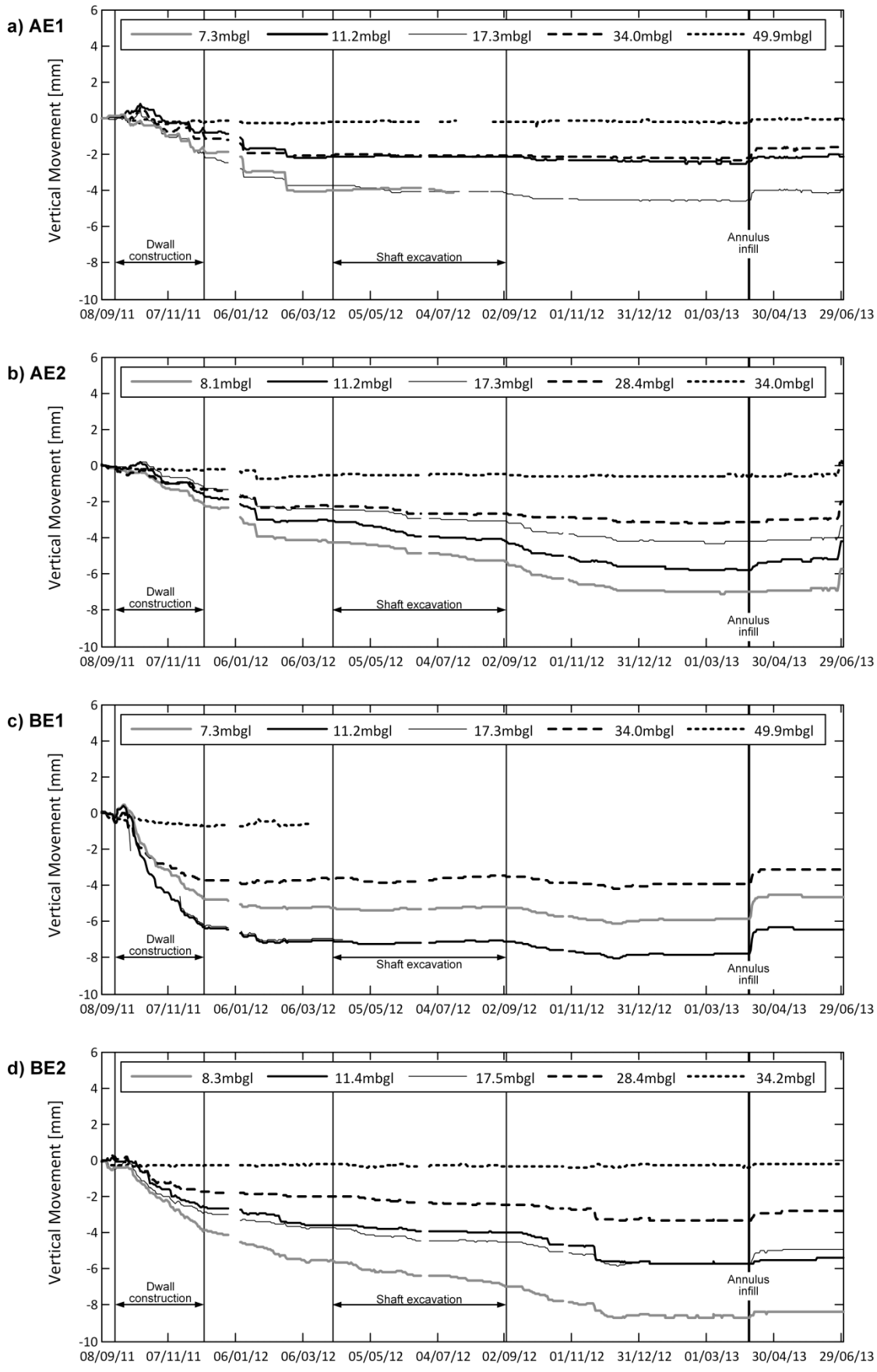

Figure 8 – Vertical movement of rod extensometer anchors (baselined with bottom anchor) for a) AE1, b) AE2, c) BE1 and d) BE2

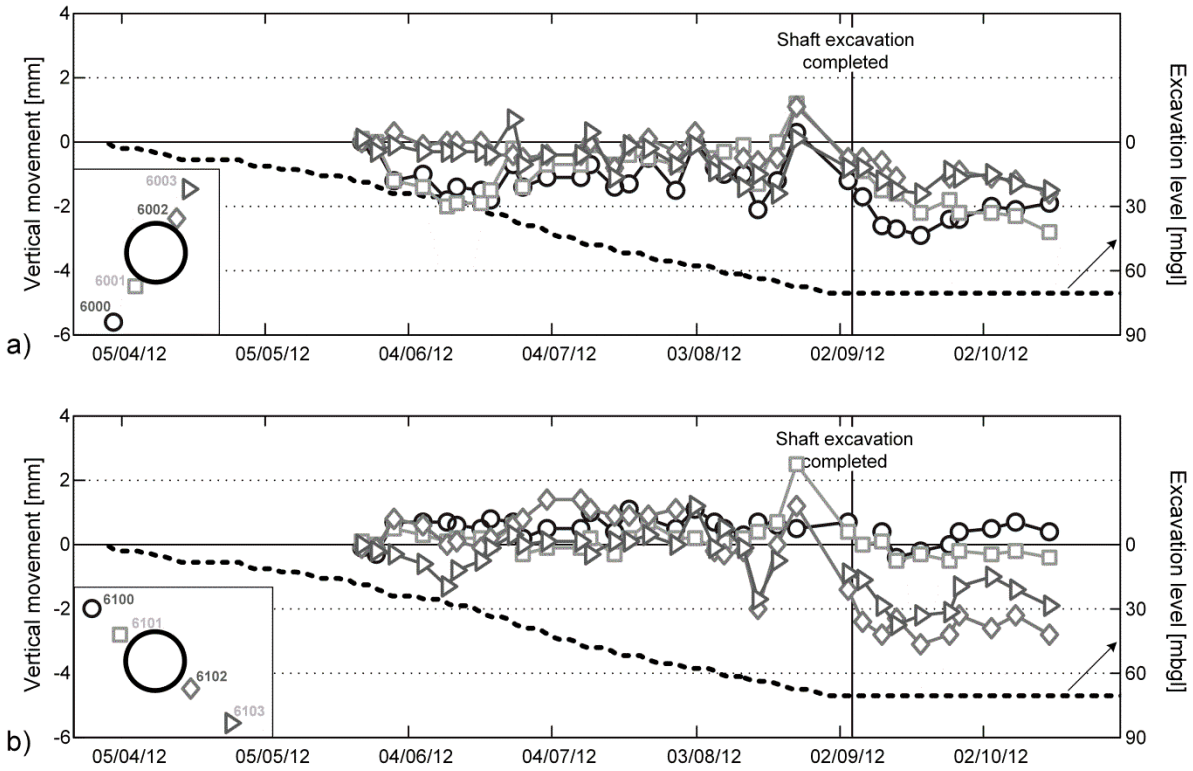

Figure 9 – Vertical movement of surface levelling pins a) Array AMA1 b) Array AMA2

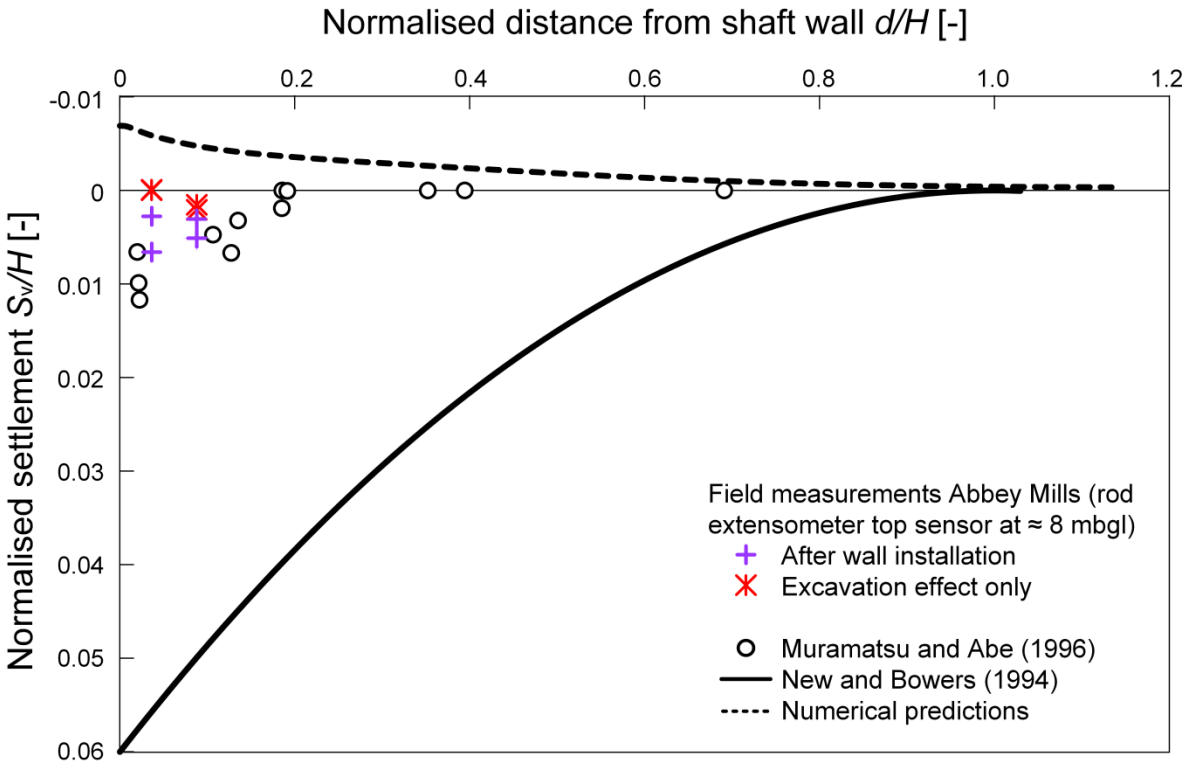

Figure 10 – Comparing Abbey Mills surface settlement data with another field study (Muramatsu and Abe, 1994), empirical predictions (New and Bowers, 1996) and numerical results (settlement is positive, heave is negative)

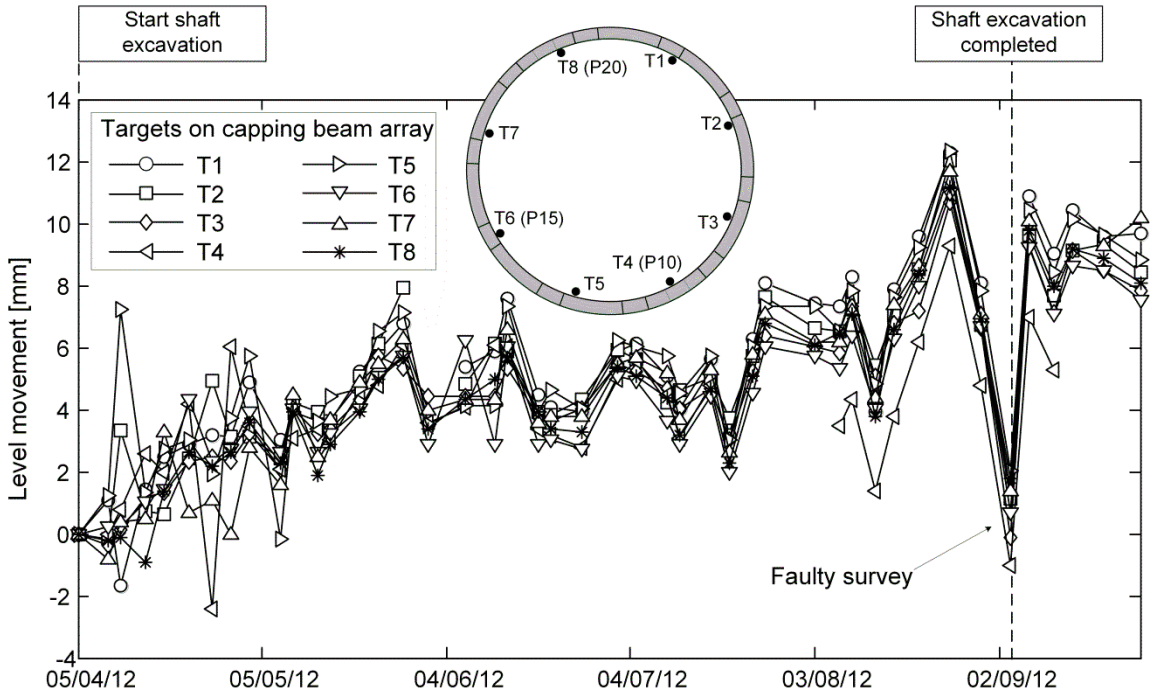

Figure 11 – Diaphragm wall survey: level movement of capping beam targets

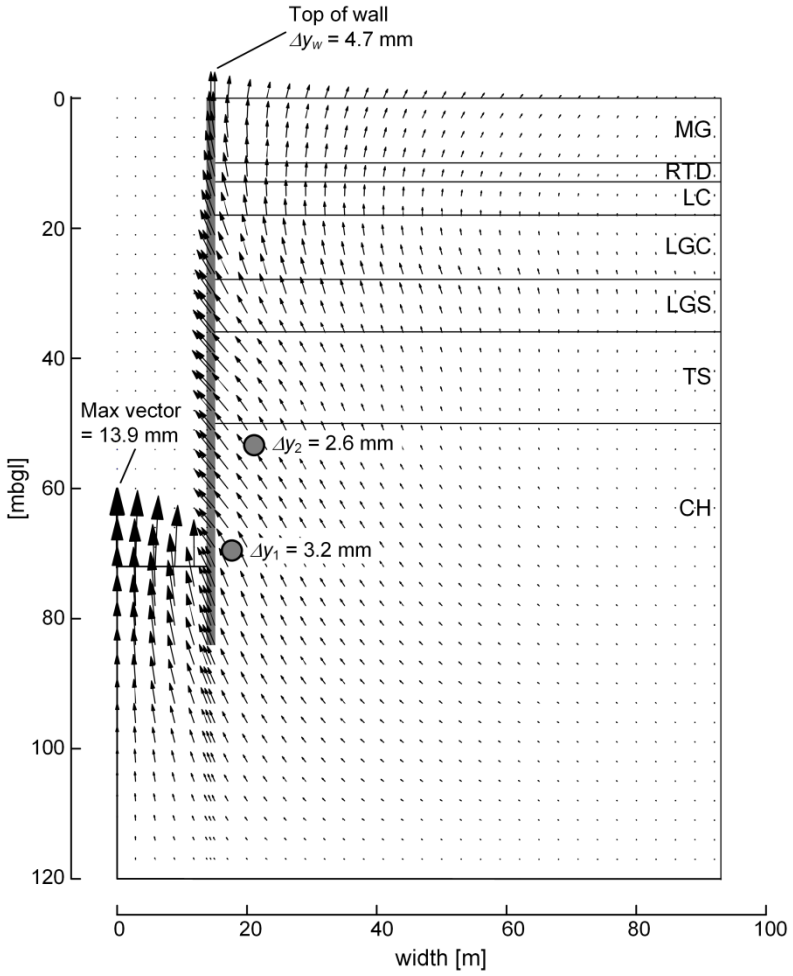

Figure 12 – FLAC2D vector plot showing excavation induced ground movement at final excavation level

Table 1 – FLAC2D input parameters for constitutive models

Strata	Soil model	Top level [mbgl]	γ_{dry} [kg/m^3]	Porosity [-]	Permeability [m/s]	K [MPa]	G [MPa]	ν [-]	ϕ' [º]	ψ [º]	c' [kPa]	K_0 [-]	a [-]
MG	MC	0	1654	0.35	1.E-05	4.2	1.9	0.3	30	0	0	0.5	-
RTD	MC	10	1654	0.35	1.E-05	41.3	19.2	0.3	38	19	0	0.6	-
LC	MC*	13	1583	0.42	1.E-08	107	80	0.2	25	0	0	1	4500
LGC	MC*	18	1642	0.36	1.E-08	666.7	500	0.2	27	0	0	1	18000
LGS	SHS	28	1654	0.35	1.E-06	44.4	33.3	0.2	40**	0**	0	1	-
TS	SHS	36	1754	0.35	1.E-06	187.5	86.5	0.2	40**	0**	0	1	-
CH	HB	50	1600	0.35	1.E-06	1000	600	0.25	Special HB parameters, see Schwamb and Soga (2015)			1	-

* with stiffness degradation ** Parameters change after onset of yield

where γ_{dry} is the dry density, K is the bulk modulus, G is the shear modulus, ν is the Poisson's ratio, ϕ' is the effective stress friction angle, ψ is the dilation angle, c' is the cohesion intercept, K_0 is the lateral at rest earth pressure coefficient and a is a parameter needed for the hyperbolic stiffness degradation (see Schwamb and Soga, 2015)